THE JOURNAL OF PHYSICAL CHEMISTRY Letters

Letter

Cite This: J. Phys. Chem. Lett. 2019, 10, 5519−5529

pubs.acs.org/JPCL

Investigating New Reactivities Enabled by Polariton Photochemistry

Arkajit Mandal and Pengfei Huo*

Department of Chemistry, University of Rochester, 120 Trustee Road, Rochester, New York 14627, United States

Supporting Information

ABSTRACT: We perform quantum dynamics simulations to investigate new chemical reactivities enabled by cavity quantum electrodynamics. The quantum light−matter interactions between the molecule and the quantized radiation mode inside an optical cavity create a set of hybridized electronic−photonic states, so-called polaritons. The polaritonic states adapt the curvatures from both the ground and the excited electronic states, opening up new possibilities to control photochemical reactions by exploiting intrinsic quantum behaviors of light−matter interactions. With quantum dynamics simulations, we demonstrate that the selectivity of a model photoisomerization reaction can be controlled by tuning the photon frequency of the cavity mode or the light−matter coupling strength, providing new ways to manipulate chemical reactions via the light−matter interaction. We further investigate collective quantum effects enabled by coupling the quantized radiation mode to multiple molecules. Our results suggest that in the resonance case, a photon is recycled among molecules to enable multiple excited state reactions, thus effectively functioning as a catalyst. In the nonresonance case, molecules emit and absorb virtual photons to initiate excited state reactions through fundamental quantum electrodynamics processes. These results from quantum dynamics simulations reveal basic principles of polariton photochemistry as well as promising reactivities that take advantage of intrinsic quantum behaviors of photons.

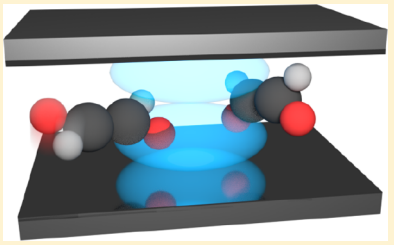

Coupling molecules to a quantized radiation field inside an optical cavity creates a set of photon-matter hybrid states, so-called polaritons. These polariton states hybridize the curvatures from both the ground and the excited electronic states and have shown a great promise to alter the photochemistry of molecules.[1−4] Unlike traditional photochemistry, which uses light as an energy source, polariton chemistry uses quantized photons as active chemical catalysts to significantly change the shape of the potential energy surface in molecular systems, and thus, open up new possibilities to tune and control chemical reactions.[5−8]

Theoretical investigations play a vital role in understanding the fundamental limits and the basic principle of new chemical reactivities achieved by polariton chemistry.[7−10] It has been shown that the presence of the cavity can suppress[11] or enhance[8,12] photoisomerizations,[11−13] increase charge transfer rates by orders of magnitude,[14−16] modify potential energy landscapes even with no photon in the cavity,[8,11,17−19] enhance electron−phonon coupling strength,[20] accelerate singlet fission kinetics,[21] remotely control chemical reactions,[22] enhance excitation energy transfer processes,[16,23,24] and create new polariton induced conical intersections.[8,18,25,26]

All of these emerging features of the polariton chemistry demonstrate a great promise to control and tune chemical reactivities, as the cavity quantum electrodynamics (QED) processes take advantage of the quantum nature of the light and its interaction with the molecular system. What remains to be done, however, is the direct quantum dynamics simulation that confirms these interesting mechanistic hypotheses and provides a time-dependent insight into these polariton mediated photochemical reactivities. Simulating the time-dependent polariton quantum dynamics of such hybrid matter−field systems is an essential task, as these polariton photochemical reactions often involve a complex dynamical interplay between the electronic, nuclear, and photonic degrees of freedom. Despite encouraging recent progress,[9,17,19,27−30] the polariton nonadiabatic dynamics remains to be clarified, which is beyond the usual paradigm of photochemistry that does not include the quantum state of photon nor explicitly consider spontaneous emission, or quantum optics that does not study molecules.

In this Letter, we perform quantum dynamics simulations to investigate the nonadiabatic transitions in a molecule−cavity hybrid system. We describe the quantized photon mode with its Fock states and explicitly treat the polaritonic nonadiabatic transitions through an accurate real-time path-integral approach. With a cavity photoisomerization model, our quantum dynamics results suggest that the reaction outcome can be controlled by tuning the photon frequency of the cavity mode, or the light−matter coupling strength, confirming the recently proposed mechanisms of manipulating chemical reactions via quantum light−matter interactions.[8,12,17] Further, we perform quantum dynamics simulations to investigate new reactivities enabled by exchanging real and virtual photons among many molecules inside the cavity. Through quantum dynamics simulations, this work demonstrates the possibilities to exploit intrinsic quantum behaviors of photons to enable new photochemical phenomena.

Received: June 3, 2019
Accepted: September 1, 2019
Published: September 1, 2019

DOI: 10.1021/acs.jpclett.9b01599
J. Phys. Chem. Lett. 2019, 10, 5519−5529

Theory and Model. We use the generalized Rabi model[31−34] to describe the molecule−cavity hybrid system.[10,11,17,26,28,29] The molecule−cavity interaction is described by the quantum electric-dipole Hamiltonian, which is obtained with the Göppert-Mayer gauge[35] (also commonly referred as the length gauge,[36] electric-dipole gauge, or power-Zienau transformation[31−33]), and the long-wavelength approximation[36] by assuming that the dimension of a molecule is much smaller than the dimensions of the optical cavity. This gives rise to the Pauli-Fierz (PF) nonrelativistic QED Hamiltonian,[30,36,37] which has been recently used to investigate cavity QED mediated photochemistry.[9,30,38] Dropping the dipole self-energy terms (which does not play a role in the model studied here) and the permanent dipole terms (which are not considered in this study) results in the following generalized Rabi model.[17,30,36,37]

The total Hamiltonian for the molecule−cavity hybrid system is expressed as[17]

$$\hat{H} = \hat{H}_e + \hat{H}_{sb} + \hat{H}_p + \hat{H}_{ep} \tag{1}$$

where $\hat{H}_e + \hat{H}_{sb}$ is the molecular Hamiltonian, $\hat{H}_p$ is the Hamiltonian of the quantized photon mode inside the cavity, and $\hat{H}_{ep}$ describes the molecule−photon interaction.

The electronic Hamiltonian $\hat{H}_e$ is described by a model system that undergoes isomerization reaction[12]

$$\hat{H}_e = \hat{T}_R + E_g(R)|g\rangle\langle g| + E_e(R)|e\rangle\langle e| \tag{2}$$

Here, $|\alpha\rangle \in \{|g\rangle, |e\rangle\}$ represents the electronic ground or excited state, R represents the reaction coordinate, and $\hat{T}_R$ is the nuclear kinetic energy operator associated with R. The detailed expression of $E_\alpha(R)$ is provided in the Supporting Information. To clearly demonstrate the quantum dynamics from the light−matter interaction, we choose to omit[12] the nonadiabatic coupling $\langle g|\nabla_R|e\rangle$ in our model system, thus effectively turning off the electronic nonadiabatic transitions between the $|g\rangle$ and $|e\rangle$ states. With this assumption, both $|g\rangle$ and $|e\rangle$ states effectively become diabatic states. In the Supporting Information, we have also tested the effects of the electronic nonadiabatic coupling (NAC) on polariton quantum dynamics. Qualitatively same results are obtained when NAC is included, suggesting a less important role of nonradiative relaxations in the polariton quantum dynamics investigated in this particular model system. This is because the NAC will not couple the photon-dressed states that have different numbers of photons; this will be discussed in detail after we introduce the polariton states in this section.

Compared to the model system used in the previous study of photoisomerization in a cavity,[12] here, we include an additional phonon bath to describe the vibrational relaxations in a molecular system. The reaction coordinate R is coupled to these vibrational modes $\mathbf{r} = \{r_k\}$ in the molecule, modeled by the following system−bath Hamiltonian

$$\hat{H}_{sb} = \hat{T}_\mathbf{r} + \sum_k \frac{1}{2}\omega_k^2\left[r_k + \frac{c_k R}{\omega_k^2}\right]^2 \tag{3}$$

In the above equation, $\hat{T}_\mathbf{r}$ represents the kinetic energy of the phonon modes and r_k is the kth phonon mode with the corresponding coupling constant c_k and frequency ω_k. The details of the bath parameters and the spectral density discretization procedure are provided in the Supporting Information.

The quantized radiation mode inside the optical cavity is described as

$$\hat{H}_p = \hbar\omega_c\left(\hat{a}^\dagger\hat{a} + \frac{1}{2}\right) = -\frac{\hbar^2}{2}\frac{d^2}{dq^2} + \frac{1}{2}\omega_c^2\hat{q}^2 \tag{4}$$

where $\hat{a}^\dagger$ and $\hat{a}$ are the photon creation and annihilation operators, respectively, and the photon displacement coordinate is $\hat{q} = \sqrt{\frac{\hbar}{2\omega_c}}(\hat{a} + \hat{a}^\dagger)$.

The light−matter interaction between the electronic and photonic DOF is expressed as

$$\hat{H}_{ep} = \hbar g_c(\hat{a} + \hat{a}^\dagger)(\hat{\sigma}^\dagger + \hat{\sigma}) = g_c\sqrt{2\hbar\omega_c}\,\hat{q}(|e\rangle\langle g| + |g\rangle\langle e|) \tag{5}$$

Here, $\hat{\sigma}^\dagger = |e\rangle\langle g|$ and $\hat{\sigma} = |g\rangle\langle e|$ are the molecular excitonic creation and annihilation operators, respectively.

The light−matter interaction strength is

$$\hbar g_c = \boldsymbol{\mu}_{eg}\cdot\hat{\mathbf{e}}\sqrt{\frac{\hbar\omega_c}{2V_c\epsilon_0}} \tag{6}$$

where $\boldsymbol{\mu}_{eg}$ is the transition dipole moment vector between electronic states $|g\rangle$ and $|e\rangle$, $\hat{\mathbf{e}}$ represents the unit vector along the direction of the cavity polarization mode, and V_c is the active volume of the cavity mode. Compared to the widely used Jaynes−Cummings model,[39] the Rabi Hamiltonian does not make the rotating-wave approximation (RWA) that ignores $\hat{a}\hat{\sigma}$ and $\hat{a}^\dagger\hat{\sigma}^\dagger$ terms.[31−34] Here, we treat $\hbar g_c$ as a constant for all of the results presented in the main text. In the Supporting Information, we also explored a more general position-dependent coupling strength $g_c(R)$, which provide qualitatively the same results obtained from the constant $\hbar g_c$ model, agreeing with the previous theoretical study.[11]

Further, we emphasize that, in general, the dipole self-energy term, $\hbar g_c^2/\omega_c$ (which is ignored in the Rabi Hamiltonian in eq 1) should be included in order to guarantee a bounded ground state of the molecule−cavity hybrid system.[36] The self-dipole term is also shown to have an important effect in the ultrastrong light−matter coupling scenario (when $g_c/\omega_c > 1.0$ in a cavity Shin−Metiu model[9]). Here, for the constant $\hbar g_c$ model presented in this study, the dipole self-energy provides the same constant energy shift for all polariton states and thus does not influence the quantum dynamics. For the position-dependent coupling model with $g_c(R)$ presented in the Supporting Information, including the self-dipole term does not quantitatively change the results, due to the intermediate coupling strength used here ($g_c/\omega_c < 0.05$), agree with recent theoretical investigations.[29]

We further denote the polariton Hamiltonian $\hat{H}_{pl}$ as follows

$$\hat{H}_{pl} = \hat{H} - \hat{T}_R - \hat{H}_{sb} = (\hat{H}_e - \hat{T}_R) + \hat{H}_p + \hat{H}_{ep} \tag{7}$$

which includes the electronic part of the molecular Hamiltonian, the kinetic and potential energy of the quantized photon mode, as well as the interaction between the molecular and photonic DOFs. Representing the radiation field in its Fock state (the photon number state), and the molecule in its electronic states, the polariton Hamiltonian $\hat{H}_{pl}$ is expressed as

DOI: 10.1021/acs.jpclett.9b01599
J. Phys. Chem. Lett. 2019, 10, 5519−5529

$$\hat{H}_{\mathrm{pl}} = \sum_{\alpha n}\left(E_{\alpha}(R) + \left(n+\frac{1}{2}\right)\hbar\omega_{\mathrm{c}}\right)|\alpha, n\rangle\langle\alpha, n| + \sum_{n}\sqrt{n+1}\,g_{\mathrm{c}}(\hat{\sigma}^{\dagger}+\hat{\sigma})(|n\rangle\langle n+1| + |n+1\rangle\langle n|) \tag{8}$$

where $|\alpha, n\rangle = |\alpha\rangle \otimes |n\rangle$ is the electronic−photonic basis (or exciton-Fock basis, photon-dressed electronic state), with $|\alpha\rangle \in \{|\mathrm{g}\rangle, |\mathrm{e}\rangle\}$, and $|n\rangle$ is the Fock state of the radiation mode with n photons in the cavity. The eigenstate of $\hat{H}_{\mathrm{pl}}$ is so-called the polariton state, which satisfies the following eigenequation

$$\hat{H}_{\mathrm{pl}}|\Phi_{\mu}(R)\rangle = E_{\mu}(R)|\Phi_{\mu}(R)\rangle \tag{9}$$

The polariton states $|\Phi_{\mu}(R)\rangle$ can be expressed as linear combinations of the exciton-Fock basis

$$|\Phi_{\mu}(R)\rangle = \sum_{\alpha,n} c^{\mu}_{\alpha n}(R)|\alpha, n\rangle \tag{10}$$

The polariton energies and eigenvectors can be obtained by diagonalizing $\hat{H}_{\mathrm{pl}}$'s matrix under the $\{|\alpha, n\rangle\}$ basis. The above procedure is completely general and can be easily extended to real molecular systems,[37] such as using *ab initio* electronic structure calculations to obtain adiabatic states $\{|\alpha(R)\rangle\}$, adiabatic energy $E_{\alpha}(R)$, and the transition dipole $\mu_{\alpha\beta}(R)$ in order to provide the on-the-fly polariton potential energy surfaces.[27−29]

For the quantum dynamics simulation of a single molecule coupled to the cavity, the initial excitation is chosen to be $|\mathrm{e}, 0\rangle$ state, which is directly coupled to the $|\mathrm{g}, 1\rangle$ state through the $\hat{a}\hat{\sigma}^{\dagger}$ and $\hat{a}^{\dagger}\hat{\sigma}$ terms in $\hat{H}_{\mathrm{ep}}$ (eq 5). Because we do not include the nonadiabatic coupling $\langle \mathrm{g}|\nabla_R|\mathrm{e}\rangle$ in the model system, $|\mathrm{e}, 0\rangle$ does not directly couple to the $|\mathrm{g}, 0\rangle$ state. Further, $|\mathrm{e}, 2\rangle$ is coupled to the $|\mathrm{g}, 1\rangle$ state through $\hat{a}\hat{\sigma}$ and $\hat{a}^{\dagger}\hat{\sigma}^{\dagger}$ terms, with a far off-resonance energy compared to $|\mathrm{e}, 0\rangle$ and $|\mathrm{g}, 1\rangle$ states. Thus, the polariton dynamics is largely confined within the $|\mathrm{e}, 0\rangle$ and $|\mathrm{g}, 1\rangle$ Hilbert subspace in this case. This allows one to analyze the Hamiltonian in the $|\mathrm{e}, 0\rangle$ and $|\mathrm{g}, 1\rangle$ subspace, although our numerical simulation *does not make any of such assumption*. The polariton Hamiltonian within this subspace is expressed as follows

$$\hat{H}_{\mathrm{pl}} = \begin{bmatrix} E_{\mathrm{g}}(R) + \hbar\omega_{\mathrm{c}} & \hbar g_{\mathrm{c}} \\ \hbar g_{\mathrm{c}} & E_{\mathrm{e}}(R) \end{bmatrix} + \frac{1}{2}\hbar\omega_{\mathrm{c}}\mathbf{1} \tag{11}$$

where $\mathbf{1}$ is the identity operator (in this subspace) and $\frac{1}{2}\hbar\omega_{\mathrm{c}}$ is the zero-point energy of the quantized photon mode inside the cavity. The light−matter coupling $\hbar g_{\mathrm{c}}$ induces a Rabi splitting between two polariton states, given by

$$\hbar\Omega_{\mathrm{c}} = \sqrt{4\hbar^2 g_{\mathrm{c}}^{\,2} + \Delta_{\mathrm{c}}^{\,2}} \tag{12}$$

where $\Delta_{\mathrm{c}} = \hbar\omega_{\mathrm{c}} - (E_{\mathrm{e}}(R) - E_{\mathrm{g}}(R))$ is the molecule−cavity detuning. Under the *resonance* condition where $E_{\mathrm{e}}(R) - E_{\mathrm{g}}(R) = \hbar\omega_{\mathrm{c}}$, the Rabi splitting becomes $\hbar\Omega_{\mathrm{c}} = 2\hbar g_{\mathrm{c}}$. The eigenstates of the above $\hat{H}_{\mathrm{pl}}$ are the polariton states, which can be expressed as $|+\rangle = \sin\phi|\mathrm{e}, 0\rangle + \cos\phi|\mathrm{g}, 1\rangle$ and $|-\rangle = \cos\phi|\mathrm{e}, 0\rangle - \sin\phi|\mathrm{g}, 1\rangle$, where ϕ is the light−matter mixing angle, with $\phi = \frac{1}{2}\tan^{-1}(2\hbar g_{\mathrm{c}}/\Delta_{\mathrm{c}})$.

In the Supporting Information, we have investigated the effects of the derivative coupling $\langle \mathrm{g}|\nabla_R|\mathrm{e}\rangle$ on polariton quantum dynamics. We find a minimum impact from it with the model system studied here, even with a large magnitude of the derivative coupling. This is because the $|\mathrm{g}, 1\rangle$ and $|\mathrm{e}, 0\rangle$ states do not couple to each other through the derivative coupling, as they differ by 1 photon; thus, $\langle \mathrm{g}, 1|\nabla_R|\mathrm{e}, 0\rangle = \langle \mathrm{g}|\nabla_R|\mathrm{e}\rangle\cdot\langle 1|0\rangle = 0$ enforced by the orthogonality the Fock states. Further, the nonadiabatic coupling between two polariton states can be shown[18] as $\langle -|\nabla_R|+\rangle = (1-\chi)/4g_{\mathrm{c}}\cdot\nabla_R[E_{\mathrm{e}}(R) - E_{\mathrm{g}}(R)] - (\chi/\Delta_{\mathrm{c}})\cdot\nabla_R g_{\mathrm{c}}(R)$, where $\chi = \Delta_{\mathrm{c}}^{\,2}/(4g_{\mathrm{c}}^{\,2} + \Delta_{\mathrm{c}}^{\,2})$. This polariton nonadiabatic coupling only depends on the light−matter interaction and does not contain any contribution from the electronic NAC, $\langle \mathrm{g}|\nabla_R|\mathrm{e}\rangle$. Thus, electronic NAC will not directly impact the most important resonance states in the Rabi model studied here. However, they do couple the $|\mathrm{e}, 0\rangle$ and $|\mathrm{g}, 0\rangle$ states as well as $|\mathrm{e}, 1\rangle$ and $|\mathrm{g}, 1\rangle$ states (because of the common Fock states), leading to the nonradiative decay channels. We find a minimum impact of these channels on the control scheme (in terms of the quantum yield of the product) presented in this study.

For the case of many molecules coupled to a common quantized radiation mode, the total Hamiltonian for the molecules−cavity hybrid system is given by

$$\hat{H} = \sum_{\nu}\hat{H}_{\mathrm{e}}(R_{\nu}) + \hat{H}_{\mathrm{sb}}(R_{\nu}, \mathbf{r}_{\nu}) + \hat{H}_{\mathrm{p}}(\hat{q}) + \sum_{\nu}\hat{H}_{\mathrm{ep}}(\sigma_{\nu}^{\dagger}, \sigma_{\nu}, \hat{q}) \tag{13}$$

where $\hat{H}_{\mathrm{g}}(R_{\nu}) + \hat{H}_{\mathrm{sb}}(R_{\nu},\mathbf{r}_{\nu})$ is the νth molecule's Hamiltonian (eq 2), $\hat{H}_{\mathrm{p}}$ is the Hamiltonian of the quantized photon mode (eq 4), and $\hat{H}_{\mathrm{ep}}(\sigma_{\nu}^{\dagger},\sigma_{\nu},\hat{q})$ describes the interaction between the photon mode $\hat{q}$ and the νth molecule (eq 5). This model can be viewed as a generalization of the Tavis−Cummings model (also referred as the Dicke model)[10,40,41] in quantum optics. To clearly demonstrate the essential feature of the collective behavior, we consider the case of two molecules coupled to one quantized radiation mode in this work. The above Hamiltonian is evaluated in the electronic−photonic basis $|\alpha, \gamma, n\rangle$, where $|\alpha\rangle$ and $|\gamma\rangle$ denote the electronic state of the first and second molecule, respectively, and $|n\rangle$ denotes the Fock state of the quantized mode inside the cavity.

In this study, we do not include the decay mechanism that accounts for cavity loss. The decay rate, $\hbar\Gamma_{\mathrm{c}}$ is related to the cavity finesse. The strong coupling regime is usually referred to as $\hbar\Omega_{\mathrm{c}} > \hbar\Gamma_{\mathrm{c}}$ (more generally, it refers to a Rabi frequency higher than all decay rates of polariton). While the typical cavity photon lifetime in a cavity is around 100 fs,[42−44] recent experimental setup has indicated a polariton lifetime of 100 ps[45−47] in a high quality cavity, which far exceeds the typical nuclear relaxation time presented in these studies. In addition, during the polariton photochemistry events, there will be multiple interconversions between the electronic excitation in molecules and photonic excitation in the cavity. Once the excitation is localized on the molecule, it is robust to the photonic loss.[29] Further, for the polariton quantum dynamics presented here, the wavepacket transiently travels on the photon dressed state to alter the course of chemical reactions. The transient presence of the photon inside the cavity can also significantly reduce the cavity loss. The influence of the cavity loss on polariton quantum dynamics will subject to future investigations, although we do not expect a major impact on the isomerization reaction.[29]

To simulate polariton quantum dynamics, we extend the utility of quantum dynamics approaches (that were originally

DOI: 10.1021/acs.jpclett.9b01599
J. Phys. Chem. Lett. 2019, 10, 5519−5529

developed for molecular systems) to describe the nonadiabatic transitions among polariton states (i.e., the electron−photon hybridized states).[17−19,27−30] In particular, we apply the partial linearized density matrix (PLDM) path-integral approach[48,49] to propagate the quantum dynamics of the molecule−cavity hybrid system. PLDM is an approximate real-time path-integral method that has been successfully applied to investigate various nonadiabatic processes.[50−54] A brief summary of this approach, together with the numerical details of the simulations are provided in the Supporting Information. Here, we apply the PLDM approach to simulate the nonadiabatic dynamics in a cavity photoisomerization model. It is also possible to use the PLDM approach with *ab initio* on-the-fly calculations[27−29] to simulate polariton quantum dynamics in a realistic molecule−cavity hybrid system, through the recently developed quasi-diabatic propagation scheme.[54−56] Other recently developed theoretical approaches, such as the quantum-electrodynamical density-functional theory (QEDFT)[57−59] or Ehrenfest+R approach[60,61] should also be ideal for such investigations.

In this Letter, we compute the time-dependent reduced density matrix of the light−matter hybrid system

$$\rho_{ij}(t) = \mathrm{Tr}_{R,\mathbf{r}}[\hat{\rho}(0)e^{i\hat{H}t/\hbar}|i\rangle\langle j|e^{-i\hat{H}t/\hbar}] \tag{14}$$

In the above expression, $\hat{H}$ is the total Hamiltonian (eq 1), and $\mathrm{Tr}_{R,\mathbf{r}}$ represents the trace over the nuclear DOF, including the reaction coordinate R and the bath coordinate $\mathbf{r}$. In addition, $\{|i\rangle, |j\rangle\} \in \{|\alpha, n\rangle\}$ for the single molecule case, and in the two molecule case $\{|i\rangle, |j\rangle\} \in \{|\alpha, \gamma, n\rangle\}$. We further compute the time-dependent population of the cis isomer state, defined as $|\mathrm{C}\rangle\langle\mathrm{C}| \equiv 1 - h(R-R_0)$, and the trans states $|\mathrm{T}\rangle\langle\mathrm{T}| \equiv h(R-R_0)$, correspondingly. Here, $h(R-R_0)$ is the Heaviside function, and $R_0 = -0.045$ au that corresponds to both the maximum of $E_g(R)$ and the minimum of $E_e(R)$ is chosen to be the dividing surface of the reaction.[12] The time-dependent population of the I isomer (C or T) is computed as

$$P_I(t) = \mathrm{Tr}_{R,\mathbf{r}}[\hat{\rho}(0)e^{i\hat{H}t/\hbar}|I\rangle\langle I|e^{-i\hat{H}t/\hbar}] \tag{15}$$

The yield of the isomer I is defined as

$$Y_I = \lim_{t\to t_p} P_I(t) \tag{16}$$

where t_p is the plateau time of the population $P_I(t)$. For the model system investigated in this study, $t_p \approx 5-10$ ps. The details of the numerical simulations are provided in the Supporting Information.

Figure 1 presents the model system and demonstrates the basic principle of polariton photochemistry. Figure 1a depicts the potential of $\hat{H}_{pl}$ (eq 8) in the electronic−photonic basis $\{|\alpha, n\rangle\}$, where $|g, 0\rangle$ (black) and $|e, 0\rangle$ (blue) represent the ground and excited states of the molecule with zero photons (vacuum state) in the cavity, and $|g, 1\rangle$ (red) represents a photon dressed state, where the molecule is in the ground electronic state and the cavity contains one photon. Thus, $|g, 1\rangle$ adapts the potential of the molecular ground state, with a vertical energy shift with the photon frequency, which is $\hbar\omega_c$ = 2.18 eV in this particular example.

Figure 1b depicts the light−matter interaction induced hybridization among the $|g, 1\rangle$ and $|e, 0\rangle$ states. Because of the transition dipole between the molecular ground $|g\rangle$ and excited $|e\rangle$ states, the $|g, 1\rangle$ and $|e, 0\rangle$ states are coupled to each other through the light−matter interaction Hamiltonian $\hat{H}_{ep}$ (eq 5)

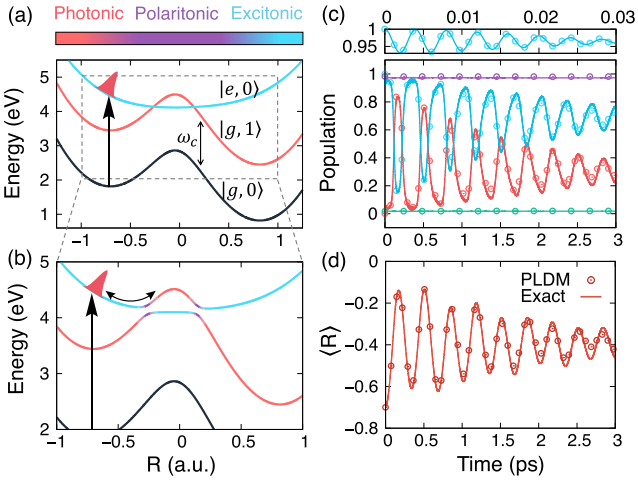

Figure 1. Polariton Hamiltonian $\hat{H}_{pl}$ in (a) the electronic−photonic basis $\{|\alpha, n\rangle\}$ and (b) the polariton states $\{|\Phi_\mu(R)\rangle\}$, with the color coding (top) that represents the excitation character. Upon photoexcitation (black arrow), the wavepacket (red) is placed on the $|e, 0\rangle$ state. (c) Polariton quantum dynamics governed by $\hat{H} - \hat{H}_{sb}$ at T = 0 K. The populations of the $|e, 0\rangle$ (red) and $|g, 1\rangle$ (blue), as well as the adiabatic polariton populations $|+\rangle$ (magenta) and $|-\rangle$ (green) are obtained from the PLDM approach (open circles) and the numerically exact calculation (solid line). (d) Time-dependent expectation value of the nuclear reaction coordinate.

and hybridized to form the upper polariton state $|+\rangle$ and the lower polariton state $|-\rangle$, which are the eigenstates of $\hat{H}_{pl}$ (eq 8). The coupling strength (eq 6) between $|g, 1\rangle$ and $|e, 0\rangle$ used here is assumed to be a constant $\hbar g_c$ = 0.136 eV, which creates a large Rabi splitting between two polariton surfaces. The curves are color coded with the scheme (on top of Figure 1a) that represents the character of excitation based on the number of photons inside the cavity, $\langle\hat{a}^\dagger\hat{a}\rangle = \langle\Phi_\mu(R)|\hat{a}^\dagger\hat{a}|\Phi_\mu(R)\rangle$, where $|\Phi_\mu(R)\rangle \in \{|+\rangle, |-\rangle\}$ (see eq 10). When the excitation is purely localized on the molecule with no photon inside the cavity, $\langle\hat{a}^\dagger\hat{a}\rangle = 0$, and the character of the excitation is purely excitonic (blue). Conversely, when the excitation is purely localized on the radiation mode inside the cavity (i.e., molecule is in the ground electronic state and the cavity contains 1 photon), $\langle\hat{a}^\dagger\hat{a}\rangle = 1$, and the character of excitation is purely photonic (red). When the energies of $|g, 1\rangle$ and $|e, 0\rangle$ are in resonance ($E_e(R) - E_g(R) \approx \hbar\omega_c$), the light−matter interaction ($\hat{H}_{ep}$ in eq 5) causes a strong mixing of the two states and a splitting (avoided crossings) between them. The resulting polariton states, which are hybrid excitations of both the molecule and the cavity (magenta), adapt a value of average photon $\langle\hat{a}^\dagger\hat{a}\rangle$ between 0 and 1. Thus, depending on the nuclear position R, the character of the excitation for the hybrid system can be excitonic (blue), photonic (red), or polaritonic (magenta).

Figure 1c presents the polariton quantum dynamics obtained from numerically exact split-operator method (solid lines) and the PLDM approach (open circle). Here, we consider the dynamics governed by $\hat{H} - \hat{H}_{sb}$ at T = 0 K, where the numerically exact results can be easily obtained. The initial condition is modeled as the Franck−Condon excitation from the $|g, 0\rangle$ to $|e, 0\rangle$ state, indicated by the vertical black arrow in panels a and b. The polariton wavepacket moves adiabatically (due to the large Rabi-splitting) on the upper polariton surface, as depicted by the curved arrow in panel b. This is reflected in the time-dependent polariton populations, where the upper

DOI: 10.1021/acs.jpclett.9b01599
J. Phys. Chem. Lett. 2019, 10, 5519−5529

polariton state |+⟩ (magenta) remains a unitary population, indicating no nonadiabatic transitions between the upper and the lower polariton state. However, the rapid population oscillations of the |g, 1⟩ (red) and |e, 0⟩ (blue) states reflect a change of the character of the polariton states, from excitonic to photonic and then back and forth. These processes occur by exchanging excitations between the molecule and the quantized photon mode inside the cavity, through the spontaneous emission (that the molecule emits one photon into the cavity) and the absorption (that the molecule absorbs one photon from the cavity and gets electronically excited). The population of |g, 1⟩ (red curve in Figure 1c) also indicates the time-dependent expected number of photons inside the cavity, which clearly demonstrates the alternating emission and absorption processes. It is worth noting that spontaneous emission is usually induced due to the vacuum fluctuations from other noncavity modes.[31−34] Here, it is induced due to the molecular vibration that changes the character of the polariton wave function. Further, the interconversions between the electronic excitation in molecule and photonic excitation in the cavity help to protect against the cavity loss, because the |e, 0⟩ state contains 0 photons and is free from the photon loss.[29] This gives rise to a much longer polariton lifetime compared to the typical lifetime of a photon, as observed in both experiments[1] and theoretical simulation.[29] Finally, we emphasize that the low frequency oscillations of |g, 1⟩ and |e, 0⟩ populations (with a period of ∼0.35 ps) are induced by changes of the polariton wave function character due to the nuclear dynamics. This can be clearly seen from the oscillatory motion of the nuclear position presented in panel d. The Rabi oscillations[31−34] (in quantum optics), however, have a much higher frequency (Ω_c in eq 12 at a particular R) and show up as fine structures in the population dynamics. On top of Figure 1c, we present the short time population of |e, 0⟩ states during the first 0.03 ps of the dynamics (with the oscillation period of ∼4 fs), corresponding to the early time fine structures of the population dynamics in panel c.

Figure 1d presents the time-dependent expectation value of the nuclear position ⟨R⟩ obtained from the numerically exact result (solid line) and PLDM (open circles). The adiabatic motion of the wavepacket on the upper polariton surface results in an oscillatory behavior of ⟨R⟩. This motion of R also changes the character of the polariton state, causing the oscillatory populations in panel c. In Figure 1c,d, PLDM provides nearly identical results compared to the numerically exact approach, demonstrating the accuracy of using such approach to simulate the polariton quantum dynamics. We will use it to explore new chemical reactivities enabled by quantum light−matter interactions in the rest of this study.

Figure 2 demonstrates the control of chemical reactivities by changing the frequency of the photon $\hbar\omega_c$ inside the cavity, with a strong light−matter coupling strength $\hbar g_c$ = 0.136 eV, such that $\beta\hbar\Omega_c \gg 1$, where $\beta = 1/k_BT$ corresponds to 300 K in this study. The initial excitation is chosen as |e, 0⟩. The schematic illustration of the dynamics for an isolated molecular system is presented in Figure 2a, whereas the schematics of the polariton dynamics for the molecule−cavity hybrid system at two different photon frequencies are presented in Figure 2b,c. The yield (eq 16) of the cis and trans isomer as a function of the photon frequency $\hbar\omega_c$ are presented in Figure 2d. The corresponding time-dependent polariton population dynamics, as well as the trans state populations are provided in the Supporting Information.

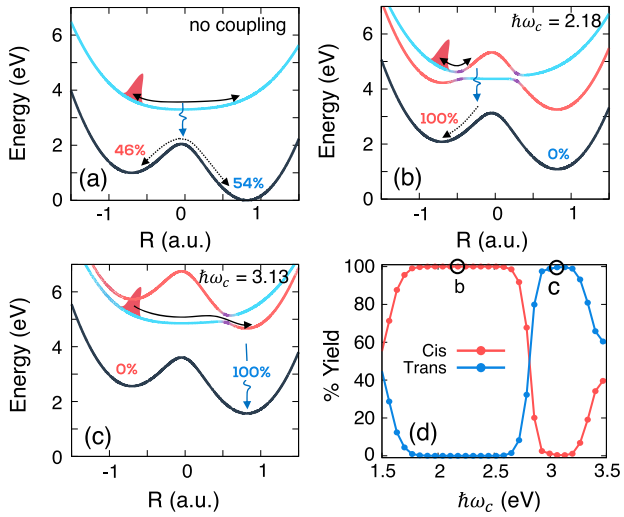

Figure 2. Control of the reactivities by changing the photon frequency $\hbar\omega_c$. Schematic illustrations of the polariton quantum dynamics are presented for (a) the bare molecular system and (b) and (c) the molecule−cavity hybrid system at various photon frequencies. (d) Quantum yield of the cis and trans isomers as a function of $\hbar\omega_c$.

In Figure 2a, the photoexcited initial wavepacket in the bare molecular system can freely explore the relatively flat |e, 0⟩ surface along the reaction coordinate R. Due to the presence of other vibrational modes (described by $\hat{H}_{sb}$ in eq 3) serving as the dissipative bath, the wavepacket eventually relaxes. Through the nonradiative decay channels (i.e., nonadiabatic coupling ⟨e|∇_R|g⟩ which is not modeled in our study) between the |e⟩ and |g⟩ state, the system relaxes back to the ground electronic state |g⟩, producing a nearly equal mixture of cis and trans isomer.

In Figure 2b, the molecule is coupled with the quantized photon mode with a frequency of $\hbar\omega_c$ = 2.18 eV, causing a hybridization between the |e, 0⟩ and |g, 1⟩ states, and creating a sizable barrier that is higher than the Franck−Condon initial excitation position. As a result, the wavepacket is confined within this cavity-induced minimum on the upper polariton surface. Further, the large light−matter coupling strength $\hbar g_c$ = 0.136 eV suppresses nonadiabatic transitions between polaritonic states. The system eventually decays to the ground state |g, 0⟩ through both the radiative and nonradiative channels, leading to a nearly 100% yield of the cis isomer. This provides a robust control to suppress photochemical isomerization (from cis to the trans configuration),[8,11] as has been recently discovered experimentally.[1]

In Figure 2c, the molecule is coupled to the photon mode which has a larger frequency $\hbar\omega_c$ = 3.13 eV, and the |g, 1⟩ state is now above the position of the Franck−Condon excitation. The wavepacket thus travels adiabatically on the lower polariton surface and relaxes to the minimum at $R \approx 0.75$ au. The system eventually decays to the ground state |g, 0⟩ through radiative or nonradiative decay channels, yielding a nearly 100% trans isomer.[12]

Figure 2d presents the yield as a function of the photon frequency. The yield at two specific $\hbar\omega_c$ are circled and labeled corresponding to the schematics presented in Figure 2b,c. Between these two regimes, the initial excitation in the |e, 0⟩ state corresponds to a linear combination of |+⟩ and |−⟩ states. The wavepacket on each polariton surface moves adiabatically, resulting in both the cis conformer (for the upper polariton

DOI: 10.1021/acs.jpclett.9b01599
J. Phys. Chem. Lett. 2019, 10, 5519−5529

component) and the trans conformer (for the lower polariton component). Increasing the photon frequency ω_c > 3.5 eV drives the |e, 0⟩ state off-resonance with the |g, 1⟩ state, and |+⟩ becomes nearly identical to |e, 0⟩. As a result, the dynamics remains almost identical to the bare molecular case, leading to the nearly equal mixture of the cis and trans isomers.

We emphasize that the above control scheme utilizes the presence of dressed levels from quantum light−matter interactions and the hybridization of different potential energy curvatures from both the ground and the excited states. In that sense, it is akin to the recently proposed Stark control[62−65] that uses classical laser field. Just like the Stark control, the scheme presented here is robust to decoherence because it does not rely on the fragile coherence properties of superposition states.[62,65] The cavity QED process relies on the transient presence of the polariton states to alter the course of chemical reactions. However, the difference between the cavity QED scheme and the classical Stark control is that the former operates at the low photon limit (0−1 photon inside the cavity), whereas the latter relies on a large number of photons.[7] Finally, when the polariton wavepacket reaches the desired nuclear region of the product state, the radiative and nonradiative decay channels enforce the final selection of various isomers. Thus, the scheme presented here is at least robust to the radiative decay channel for the model system studied in this work.

The polariton quantum dynamics can also be controlled by the light−matter coupling strength $\hbar g_c$, which dictates the nonadiabaticity of the polariton quantum dynamics.[17] As we have already seen in Figures 1 and 2, the "strong coupling regime" where the large g_c causes a sizable Rabi splitting, turns off nonadiabatic transitions between polariton states and confines the wavepacket in one polariton surface.[1,2,8,11,12,66] The intermediate coupling, which is weak enough to allow nonadiabatic transitions among polariton states, but still strong enough to mix the |e, 0⟩ and |g, 1⟩ states, can potentially offer new reactivities compared to the strong coupling regime. Here, we explore such possibility by changing $\hbar g_c$. Despite existing theoretical work that has shown the effect of changing $\hbar g_c$ in a NaI-cavity system,[17] the current work demonstrates the control of chemical reactivities with *both* ω_c and $\hbar g_c$ in one consistent model isomerization system through direct quantum dynamical simulations. The coupling strength (see eq 6) can be experimentally tuned by changing (i) the effective quantization volume V_c (by changing the lateral dimensions of the mirrors in a planar Fabry−Pérot cavity[47,67]), (ii) the permittivity ϵ_0 (by changing the types of the hosting polymer[1] inside the cavity), or (iii) the relative alignment between the molecular transition dipole moment and radiation mode, which has been recently accomplished in the plasmonic nanocavity at the single-molecule level.[66]

Figure 3a,b presents the schematics of the polariton quantum dynamics with two different light−matter coupling strengths at (a) $\hbar g_c$ = 0.0271 eV and (b) $\hbar g_c$ = 0.0957 eV, respectively, with the photon frequency $\hbar\omega_c$ = 2.45 eV. The polariton dynamics in Figure 3b is adiabatic due to the large coupling strength that suppresses nonadiabatic transitions among polariton states, such that the wavepacket is confined on the cis side of the dividing surface. Figure 3a presents the polariton dynamics with an intermediate coupling strength, such that $\beta\hbar\Omega_c \approx 1$. Under this condition, the wavepacket branches to the trans configurations of the |g, 1⟩ and |e, 0⟩ states through nonadiabatic transitions. As a result, the

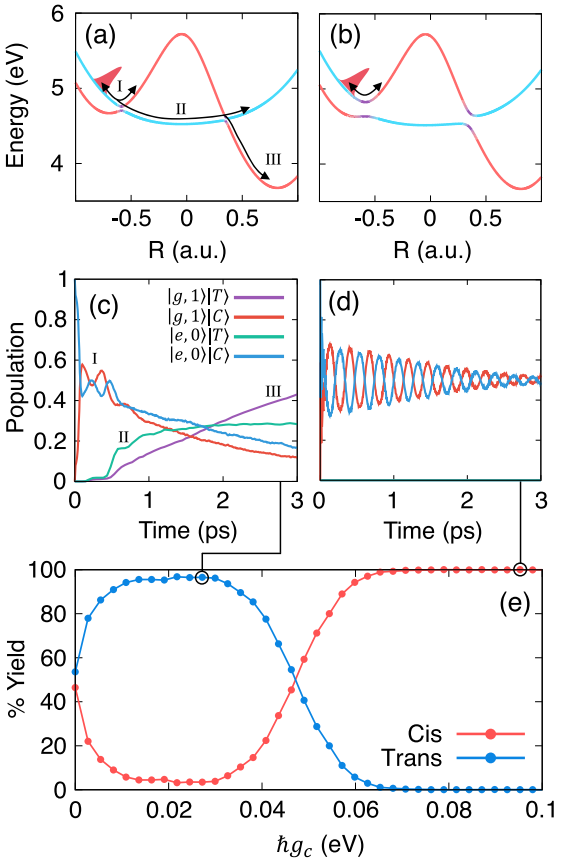

Figure 3. Control of the reactivities by changing the light−matter coupling strength $\hbar g_c$, with a fixed photon frequency ω_c = 2.45 eV. Polariton dynamics at (a) $\hbar g_c$ = 0.0271 eV and at (b) $\hbar g_c$ = 0.0957 eV, with the corresponding population dynamics provided in (c) and (d). (e) Quantum yield of the cis and trans isomers as a function of $\hbar g_c$.

molecule can access the global potential minimum of the hybrid system on the trans side of the |g, 1⟩ surface, leading to nearly 100% trans isomer for the product. This completely alters the selectivity of the product, compared to the large coupling strength scenario presented in panel b, even though the same photon frequency is used.

Figure 3c,d presents the population dynamics of the conformation specific states |e, 0⟩|C⟩, |g, 1⟩|C⟩, |e, 0⟩|T⟩, and |g, 1⟩|T⟩, corresponding to the schematics presented in Figure 3a,b. The oscillations between |e, 0⟩|C⟩ and |g, 1⟩|C⟩ states in Figure 3d reflect the adiabatic dynamics on the upper polariton surface |+⟩, similar to those presented in Figure 1. Meanwhile, |e, 0⟩|T⟩ and |g, 1⟩|T⟩ states remain unpopulated, as the wavepacket is adiabatically confined on the cis conformer side of the upper polariton surface. However, Figure 3c shows several interesting features of the population dynamics, which can be characterized into three stages. In stage I, the wavepacket moves to the light-induced avoided crossing at $R \approx 0.5$ au, causing the change of the character of the polariton wave function, and the oscillations between |e, 0⟩|C⟩ and |g, 1⟩|C⟩ in a short period of time (≈300 fs). This is followed by a sharp population increase of |e, 0⟩|T⟩ in stage II, as the wavepacket undergoes nonadiabatic transitions between the upper and lower polariton surfaces and across the dividing surface (R_0 = −0.045 au) of the isomerization reaction on the |e, 0⟩ state. Finally, in stage III, a steady increasing |g, 1⟩|T⟩

DOI: 10.1021/acs.jpclett.9b01599
J. Phys. Chem. Lett. 2019, 10, 5519−5529

population indicates the nonadiabatic transitions between the upper and lower polariton surfaces at $R \sim 0.4$ au, leading to the trans isomer. These three stages of the population dynamics are labeled in panels a and c. During this process, the hybrid matter–field system experiences a rich dynamical interplay among the electronic, nuclear, and photonic DOFs. Its excitation character starts with a molecular exciton, then changes to polariton and back to exciton (during I to II), and changes again to polariton and finally to an almost photonic excitation (during II to III). Thus, inside such a molecule–cavity hybrid system, the motion of the nuclei significantly impacts the quantum state of the photon as well as the nature of the excitation. However, the time-dependent quantum mechanical state of the photon also exerts different forces on nuclear DOF (by changing the curvature of the excited states), influencing its motion and opening up new possibilities to alter the course of chemical reactions.

Figure 3e presents the yield of the isomerization reaction by changing the light–matter coupling strength $\hbar g_c$. At a nearly zero coupling strength, the hybrid molecule–cavity system reduces to the uncoupled case, resulting in a nearly equal amount of cis and trans isomers. A small increase of $\hbar g_c$ (≈0.005 eV) significantly enhances the selectivity toward to the trans isomer, as it enables the nonadiabatic branching channels among different polariton surfaces. The trans yield reaches to nearly 100% in the range $\hbar g_c \in [0.01, 0.03]$ eV. The polariton quantum dynamics in this region corresponds to the schematic illustration in Figure 3a. Further increasing $\hbar g_c$ leads to the adiabatic polariton quantum dynamics and a switching of the selectivity for the isomerization reaction. For $\hbar g_c > 0.06$ eV, the yield of the cis isomer reaches nearly 100%, corresponding to the adiabatic dynamics presented in Figure 3b.

Figure 4 presents the polariton dynamics of the hybrid system that contains two molecules inside an optical cavity. Figure 4a presents the lower polariton surface, with the black dots indicating one of the two equivalent minimum energy paths on this surface. Both molecules are coupled to a common quantized radiation mode (through $\hat{H}$ described in eq 13). The photon frequency in this calculation is set to be $\omega_c = 2.585$ eV and it is in resonance with the excitation energy of both molecules at the position of their Franck–Condon points, such that $E_{ge0} - E_{gg0} = E_{eg0} - E_{gg0} \approx \hbar\omega_c$. The light–matter coupling strength is set to be $\hbar g_c = 0.136$ eV, causing a large Rabi splitting between different polariton states. The initial photoexcitation is prepared on the lower polariton state of the molecule–cavity system by a vertical photoexcitation from the ground state $|g, g, 0\rangle$ at the cis nuclear configurations for both molecules.

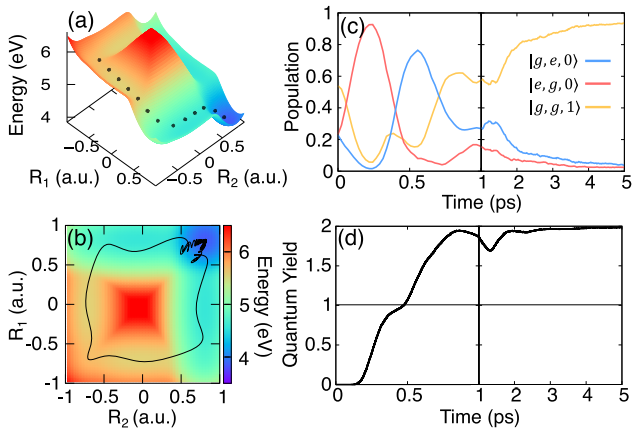

Figure 4. Polariton dynamics of two molecules coupled to a resonant radiation mode. (a) Adiabatic polariton surface, with black dots indicating one of two equivalent minimum energy paths. (b) Expectation value of the nuclear position on adiabatic polariton potential. (c) Population dynamics corresponding to the upper reaction paths. (d) Time-dependent quantum yield of the trans isomer.

Figure 4b presents the reaction path specific expectation value of the reaction coordinate (black solid line) on the lower polariton surface. It is classified as molecule 1 isomerizing prior to molecule 2 (upper off-diagonal), or molecule 2 isomerizing prior to molecule 1 (lower off-diagonal). They are equivalent paths for this bimolecular reaction and are equally likely to appear in our simulation, as one expected due to the symmetry of the Hamiltonian.

Figure 4c presents the polariton population dynamics corresponding to the upper off-diagonal path in Figure 4b; i.e., molecule 1 isomerizes prior to molecule 2. The wavepacket propagates adiabatically on the lower polariton surface, following the barrierless reaction path and relaxes to the minimum that corresponds to the trans configuration of both molecules. The initial polaritonic state corresponds to a superposition of excitations on both molecules and the radiation mode, resulting in a nonzero number of photons inside the cavity. The superposition of the excitation quickly collapses onto molecule 1 during the first 200 fs, indicated by a sharp increase in the $|e, g, 0\rangle$ state population (red curve). The excited molecule 1 undergoes cis to trans isomerization, leading to a quantum yield of nearly 100% for the trans isomer at $t = 0.4$–0.5 ps (see Figure 4d). Following the isomerization of molecule 1, the hybrid molecule–cavity system releases a photon back to the cavity, indicated by an increase in the $|g, g, 1\rangle$ population at $t = 0.4$ ps (yellow curve). The photon is then immediately absorbed by molecule 2 (which was still in the cis configuration at that moment), causing the increase in the $|g, e, 0\rangle$ population at $t = 0.6$ ps (blue curve). Following this excitation, molecule 2 undergoes cis to trans isomerization and then releases the photon back to the cavity, leading to the increasing $|g, g, 1\rangle$ population at a longer time.

Figure 4d presents the time-dependent quantum yield of the trans isomer in this hybrid system. By coupling to the common quantized radiation mode, two molecules undergo chemical reactions with only one photon inside the optical cavity, leading to a quantum yield of nearly 200%. This process overcomes the Stark–Einstein limit,[8,12] which requires one photon per molecular photoreaction. With the presence of the cavity, the photon is recycled among multiple molecules, which enables excited state reactions, thus enabling the hybrid system to go beyond the Stark–Einstein limits through a novel collective excitation.[8,12] In that sense, the quantized photon is used as a *catalyst* (participate in the reaction without being consumed), as opposed to just the energy source to excite the system in traditional photochemistry. We emphasize that this mechanism has been recently hypothesized by Feist and co-workers[8,12] on the basis of analyzing polariton potential energy surfaces (cavity Born–Oppenheimer surface[9]). Here, to the best of our knowledge, we provide the *first direct quantum dynamics simulation* that confirms this mechanistic hypothesis and provides a time-dependent insight into these polariton mediated photochemical processes.

DOI: 10.1021/acs.jpclett.9b01599
J. Phys. Chem. Lett. 2019, 10, 5519–5529

Figure 5 presents the polariton dynamics with two molecules coupled to an *off-resonant* quantized radiation mode inside the optical cavity. Figure 5a presents the potential energy surfaces of the $|e, g, 1\rangle$ state (red) and $|g, e, 1\rangle$ state (blue). In this example, the photon frequency is $\hbar\omega_c = 7.62$ eV $\gg E_{ge0} - E_{gg0} = E_{eg0} - E_{gg0}$, such that the $|g, g, 1\rangle$ state (not shown in this figure) lies well above both the $|g, e, 0\rangle$ and the $|e, g, 0\rangle$ state. Further, the two molecules are not directly coupled to each other through the electronic interaction, i.e., $\langle g, e, 0|\hat{V}|e, g, 0\rangle = 0$, where $\hat{V} = \sum_\nu \hat{H}_{ep}(\sigma_\nu^\dagger, \sigma_\nu, \hat{q})$ is the light−matter interaction Hamiltonian in eq 13. However, they are both strongly coupled to the $|g, g, 1\rangle$ state, with a strength of $\hbar g_c = 0.2714$ eV. Due to these off-resonance interactions, the $|g, e, 0\rangle$ and $|e, g, 0\rangle$ states start to mix with the $|g, g, 1\rangle$ component, allowing them to effectively interact with each other. This effective coupling can be understood from the following perturbative analysis, which is not assumed in our quantum dynamics simulations. The light−matter interaction generates the perturbed state $|g, e, 0'\rangle = |g, e, 0\rangle + \hbar g_c|g, g, 1\rangle/[E_{ge0} - E_{gg1}]$, and $|e, g, 0'\rangle$ state with a similar expression. Because of the presence of the $|g, g, 1\rangle$ component, an effective coupling between these two perturbed states is

$$\langle g, e, 0'|\hat{V}|e, g, 0'\rangle = \frac{\hbar^2 g_c^{\,2}}{E_{ge0} - E_{gg1}} + \frac{\hbar^2 g_c^{\,2}}{E_{eg0} - E_{gg1}} \qquad (17)$$

Figure 5b presents the population dynamics (red and blue) as well as the time-dependent quantum yield (black). Here, the system is initially excited to the $|e, g, 0\rangle$ state. While population is transferred from the $|e, g, 0\rangle$ state (red) to the $|g, e, 0\rangle$ state (blue), the $|g, g, 1\rangle$ state (yellow) is only virtually populated (with no apparent population). The quantum yield (black) reaches a value of 1.2, higher than the Stark−Einstein limit. This process is usually referred as the "superexchange" mechanism in chemical kinetics, where the $|g, g, 1\rangle$ state is only virtually populated to facilitate the nonadiabatic transitions between the $|e, g, 0\rangle$ and $|g, e, 0\rangle$ states. This off-resonant case can significantly suppress the cavity loss, which leaks the photon population to the other noncavity modes, due to the nearly zero photonic population during the polariton dynamics. Note that this mechanism is different than the one presented in Figure 4 where the population is *sequentially* transferred between the molecular excitation and the photonic excitation. Similar sequential and superexchange mechanisms have been recently discussed in the context of singlet fission (SF),[68,69] where the charge transfer (CT) states are used as the intermediate or virtual state to connect the singlet and triplet−triplet pair states. In the context of SF, the superexchange mechanism provides a new possibility to engineer fission materials even when the CT states are off-resonance with the singlet and triplet pair states, disproving the previous belief that the CT states are only functionally relevant when they are in resonance with these states.[68,69] In a similar sense, here we demonstrate new possibilities of achieving polariton photochemical reactivities even when the cavity is off-resonance with the molecular excitation, through exchanging virtual photons between molecules and the cavity.

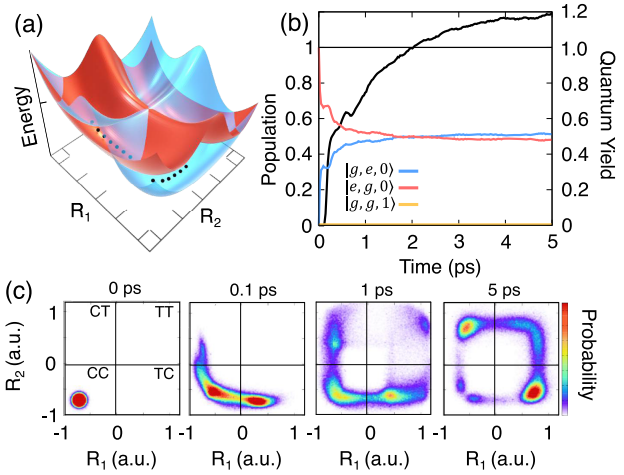

Figure 5. Polariton dynamics of two molecules coupled to an off-resonant radiation mode. (a) Potential energy surfaces of $|g, e, 0\rangle$ (blue) and $|e, g, 0\rangle$ (red) states, with black dots indicating a schematic nuclear path. (b) Population dynamics and corresponding time-dependent quantum yield. (c) Histogram of the nuclear distribution at various times during the reaction, with red represent a higher probability density.

Figure 5c presents the nuclear position distribution at various times during the polariton photochemical reaction. Four distinct regions are defined with the dividing surface at $R_i = -0.045$ au ($i = 1, 2$) along each isomerization coordinate. These regions are labeled as CC, CT, TC, and TT, where the first and the second letter indicate the configuration of the first and second molecule, respectively. The time-dependent nuclear distribution depicts the longer time nuclear configurations in each region; the overall yield of trans isomer at a longer time is higher than 100% due to the nonzero probability of the TT nuclear configuration.

To the best of our knowledge, this is the *first time* that the virtual photon has been demonstrated to mediate photochemical reactions. Similar physical processes that exchange virtual photons have been extensively discussed in the context of quantum electrodynamics and atomic quantum optics.[70−75] Here, molecules emit and absorb *virtual* photons, exerting additional forces on nuclei and altering the course of chemical reactions. This perhaps marks the fundamental difference between polariton photochemistry which in this case operates at the zero-photon limit, compared to the classical laser-matter interaction which operates at the limit with a large number of photons. In general, cavity enables the hybrid system to explore Fock states that are close to the vacuum state, opening up new possibilities that are not available or difficult to access to at the large photon number limit.[6−8]

In conclusion, we investigate the real-time polariton quantum dynamics for a model isomerization molecule coupled to an optical cavity. The quantum light−matter interactions hybridize the molecular excitation and the photonic excitation, creating a set of light−matter hybrid states, so-called the polaritons. These polariton states hybridize the curvatures from both the ground and the excited electronic states.[1,5,7,8] For such molecule−cavity hybrid system, the time-dependent quantum mechanical state of the photon exerts different forces on nuclear DOF (by changing the curvature of the polariton states), influencing its motion and thus opening up new possibilities to tune and control photochemical reactions.

Our quantum dynamics simulations demonstrate that by changing the frequency of the photon inside the cavity, one can selectively modify the polaritonic potential energy surface, allowing the wavepacket to relax to different nuclear

DOI: 10.1021/acs.jpclett.9b01599
J. Phys. Chem. Lett. 2019, 10, 5519−5529

configurations and thus control the outcome of the model isomerization reactions. Further, by tuning the light−matter coupling strength, and hence the nonadiabaticity of the polariton quantum dynamics, the wavepacket can either be confined on one polariton surface or allowed to explore multiple surfaces through nonadiabatic transitions, resulting in different preference of the product.

Further, we explore the collective behavior of molecules that stems from strong coupling to a common quantized radiation mode inside the cavity. This forms a polaritonic "super-molecule" that spans across many molecules and the cavity.[8,12] For the resonance case, our quantum dynamics results reveal a sequential transfer of the population among molecular excitonic states and the cavity photonic state, where one molecule absorbs photon and undergoes excited state isomerization reaction, emit photon back to the cavity, then the second molecule absorbs it and reacts. During this process, the photon is recycled among different molecules and the cavity, effectively serving as a *catalyst* for the photochemical reactions. In the off-resonance case, molecular excitonic states transfer population by using the off-resonant photonic state as a virtual state, thus emitting and absorbing the *virtual* photon to react. To the best of our knowledge, this is the *first time* that the virtual photon has been demonstrated to mediate photochemical reactions. Both cases lead to a quantum yield beyond the Stark−Einstein limit.

Through quantum dynamics simulations, this work reveals and clarifies several basic principles of polariton photochemistry by providing dynamic insights into cavity mediated photochemical processes. Future investigations will focus on providing the fundamental understanding of cavity quantum electrodynamics induced chemistry, as well as new reactivities that exploit intrinsic quantum behaviors of photons, facilitating the merger of quantum optics and photochemistry.

■ ASSOCIATED CONTENT

Supporting Information

The Supporting Information is available free of charge on the ACS Publications website at DOI: 10.1021/acs.jpclett.9b01599.

Details of the model Hamiltonian; details of the PLDM quantum dynamics approach; additional results of polariton dynamics with different frequencies of the photon in the cavity; results obtained when considering electronic nonadiabatic coupling and the position-dependent transition dipole (PDF)

■ AUTHOR INFORMATION

Corresponding Author

*E-mail: pengfei.huo@rochester.edu.

ORCID

Pengfei Huo: 0000-0002-8639-9299

Notes

The authors declare no competing financial interest.

■ ACKNOWLEDGMENTS

This work was supported by the National Science Foundation "Enabling Quantum Leap in Chemistry" program under a Grant number CHE-1836546. Computing resources were provided by the Center for Integrated Research Computing (CIRC) at the University of Rochester. We thank J. Sebastian Sandoval for providing the numerically exact simulations, and appreciate numerous valuable discussions with Dr. Bing Gu.

■ REFERENCES

(1) Hutchison, J. A.; Schwartz, T.; Genet, C.; Devaux, E.; Ebbesen, T. W. Modifying Chemical Landscapes by Coupling to Vacuum Fields. *Angew. Chem., Int. Ed.* **2012**, *51*, 1592−1596.

(2) Schwartz, T.; Hutchison, J. A.; Genet, C.; Ebbesen, T. W. Reversible Switching of Ultrastrong Light-Molecule Coupling. *Phys. Rev. Lett.* **2011**, *106*, 196405.

(3) Munkhbat, B.; Wersall, M.; Baranov, D. G.; Antosiewicz, T. J.; Shegai, T. Suppression of Photo-Oxidation of Organic Chromophores by Strong Coupling to Plasmonic Nanoantennas. *Sci. Adv.* **2018**, *4*, No. eaas9552.

(4) Stranius, K.; Hertzog, M.; Börjesson, K. Selective Manipulation of Electronically Excited States Through Strong Light-Matter Interactions. *Nat. Commun.* **2018**, *9*, 2273.

(5) Ebbesen, T. W. Hybrid Light-Matter States in a Molecular and Material Science Perspective. *Acc. Chem. Res.* **2016**, *49*, 2403−2412.

(6) Thomas, A.; Lethuillier-Karl, L.; Nagarajan, K.; Vergauwe, R. M. A.; George, J.; Chervy, T.; Shalabney, A.; Devaux, E.; Genet, C.; Moran, J.; Ebbesen, T. W. Tilting a Ground-State Reactivity Landscape by Vibrational Strong Coupling. *Science* **2019**, *363*, 615−619.

(7) Kowalewski, M.; Mukamel, S. Manipulating Molecules with Quantum Light. *Proc. Natl. Acad. Sci. U. S. A.* **2017**, *114*, 3278−3280.

(8) Feist, J.; Galego, J.; Garcia-Vidal, F. J. Polaritonic Chemistry with Organic Molecules. *ACS Photonics* **2018**, *5*, 205−216.

(9) Flick, J.; Ruggenthaler, M.; Appel, H.; Rubio, A. Atoms and Molecules in Cavities, from Weak to Strong Coupling in Quantum-Electrodynamics (QED) Chemistry. *Proc. Natl. Acad. Sci. U. S. A.* **2017**, *114*, 3026.

(10) Ribeiro, R. F.; Martnez-Martnez, L. A.; Du, M.; Campos-Gonzalez-Angulo, J.; Yuen-Zhou, J. Polariton Chemistry: Controlling Molecular Dynamics with Optical Cavities. *Chem. Sci.* **2018**, *9*, 6325−6339.

(11) Galego, J.; Garcia-Vidal, F. J.; Feist, J. Suppressing Photochemical Reactions with Quantized Light Fields. *Nat. Commun.* **2016**, *7*, 13841.

(12) Galego, J.; Garcia-Vidal, F. J.; Feist, J. Many-Molecule Reaction Triggered by a Single Photon in Polaritonic Chemistry. *Phys. Rev. Lett.* **2017**, *119*, 136001.

(13) Galego, J.; Garcia-Vidal, F. J.; Feist, J. Cavity-Induced Modifications of Molecular Structure in the Strong-Coupling Regime. *Phys. Rev. X* **2015**, *5*, 041022.

(14) Herrera, F.; Spano, F. C. Cavity-Controlled Chemistry in Molecular Ensembles. *Phys. Rev. Lett.* **2016**, *116*, 238301.

(15) Semenov, A.; Nitzan, A. Electron Transfer in Confined Electromagnetic Fields. *J. Chem. Phys.* **2019**, *150*, 174122.

(16) Schäfer, C.; Ruggenthaler, M.; Appel, H.; Rubio, A. Modification of Excitation and Charge Transfer in Cavity Quantum-Electrodynamical Chemistry. *Proc. Natl. Acad. Sci. U. S. A.* **2019**, *116*, 4883−4892.

(17) Kowalewski, M.; Bennett, K.; Mukamel, S. Cavity Femtochemistry: Manipulating Nonadiabatic Dynamics at Avoided Crossings. *J. Phys. Chem. Lett.* **2016**, *7*, 2050−2054.

(18) Kowalewski, M.; Bennett, K.; Mukamel, S. Non-Adiabatic Dynamics of Molecules in Optical Cavities. *J. Chem. Phys.* **2016**, *144*, 054309.

(19) Triana, J. F.; Pelez, D.; Sanz-Vicario, J. L. Entangled Photonic-Nuclear Molecular Dynamics of LiF in Quantum Optical Cavities. *J. Phys. Chem. A* **2018**, *122*, 2266−2278.

(20) Sentef, M. A.; Ruggenthaler, M.; Rubio, A. Cavity Quantum-Electrodynamical Polaritonically Enhanced Electron-Phonon Coupling and Its Influence on Superconductivity. *Sci. Adv.* **2018**, *4*, eaau6969.

(21) Martinez-Martinez, L. A.; Du, M.; Ribeiro, R. F.; Kena-Cohen, S.; Yuen-Zhou, J. Polariton-Assisted Singlet Fission in Acene Aggregates. *J. Phys. Chem. Lett.* **2018**, *9*, 1951−1957.

DOI: 10.1021/acs.jpclett.9b01599
J. Phys. Chem. Lett. 2019, 10, 5519−5529

(22) Du, M.; Ribeiro, R. F.; Yuen-Zhou, J. Remote Control of Chemistry in Optical Cavities. *Chem.* **2019**, *5*, 1167−1181.
(23) Du, M.; Martnez-Martnez, L. A.; Ribeiro, R. F.; Hu, Z.; Menon, V. M.; Yuen-Zhou, J. Theory for Polariton-Assisted Remote Energy Transfer. *Chem. Sci.* **2018**, *9*, 6659−6669.
(24) Gonzalez-Ballestero, C.; Feist, J.; Moreno, E.; Garcia-Vidal, F. J. Harvesting Excitons Through Plasmonic Strong Coupling. *Phys. Rev. B: Condens. Matter Mater. Phys.* **2015**, *92*, 121402.
(25) Bennett, K.; Kowalewski, M.; Mukamel, S. Novel Photochemistry of Molecular Polaritons in Optical Cavities. *Faraday Discuss.* **2016**, *194*, 259−282.
(26) Szidarovszky, T.; Halsz, G. J.; Csszr, A. G.; Cederbaum, L. S.; Vibk, g. Conical Intersections Induced by Quantum Light: Field-Dressed Spectra from the Weak to the Ultrastrong Coupling Regimes. *J. Phys. Chem. Lett.* **2018**, *9*, 6215−6223.
(27) Groenhof, G.; Toppari, J. J. Coherent Light Harvesting through Strong Coupling to Confined Light. *J. Phys. Chem. Lett.* **2018**, *9*, 4848−4851.
(28) Luk, H. L.; Feist, J.; Toppari, J. J.; Groenhof, G. Multiscale Molecular Dynamics Simulations of Polaritonic Chemistry. *J. Chem. Theory Comput.* **2017**, *13*, 4324−4335.
(29) Fregoni, J.; Granucci, G.; Coccia, E.; Persico, M.; Corni, S. Manipulating Azobenzene Photoisomerization Through Strong Light-Molecule Coupling. *Nat. Commun.* **2018**, *9*, 4688.
(30) Vendrell, O. Coherent Dynamics in Cavity Femtochemistry: Application of the Multi-Configuration Time-Dependent Hartree Method. *Chem. Phys.* **2018**, *509*, 55.
(31) Cohen-Tannoudji, C.; Dupont-Roc, J.; Grynberg, G. *Photons and Atoms: Introduction to Quantum Electrodynamics*; John Wiley & Sons, Inc., 1989.
(32) Grynberg, G.; Aspect, A.; Fabre, C. *Introduction to Quantum Optics: From the Semi-classical Approach to Quantized Light*; Cambridge University Press, 2010.
(33) Steck, D. A. Quantum and Atom Optics, available online at http://steck.us/teaching, 2018.
(34) Scully, M. O.; Zubairy, M. S. *Quantum Optics*; Cambridge University Press, 1999.
(35) Göppert-Mayer, M. Elementary Processes with Two Quantum Transitions. *Ann. Phys. (Berlin, Ger.)* **2009**, *18*, 466−479.
(36) Rokaj, V.; Welakuh, D. M.; Ruggenthaler, M.; Rubio, A. Light-Matter Interaction in the Longwavelength Limit: No Ground-State Without Dipole Self-Energy. *J. Phys. B: At., Mol. Opt. Phys.* **2018**, *51*, 034005.
(37) Schäfer, C.; Ruggenthaler, M.; Rubio, A. Ab Initio Nonrelativistic Quantum Electrodynamics: Bridging Quantum Chemistry and Quantum Optics from Weak to Strong Coupling. *Phys. Rev. A: At., Mol., Opt. Phys.* **2018**, *98*, 043801.
(38) Flick, L. J.; Appel, H.; Ruggenthaler, M.; Rubio, A. Cavity Born-Oppenheimer Approximation for Correlated Electron-Nuclear-Photon Systems. *J. Chem. Theory Comput.* **2017**, *13*, 1616−1625.
(39) Jaynes, E.; Cummings, F. Comparison of Quantum and Semiclassical Radiation Theories with Application to the Beam Maser. *Proc. IEEE* **1963**, *51*, 89−109.
(40) Tavis, M.; Cummings, F. Exact Solution for an N-Molecule-Radiation-Field Hamiltonian. *Phys. Rev.* **1968**, *170*, 379−384.
(41) Dicke, R. Coherence in Spontaneous Radiation Processes. *Phys. Rev.* **1954**, *93*, 99−110.
(42) Martinez-Martinez, L. A.; Du, M.; Ribeiro, R. F.; Kena-Cohen, S.; Yuen-Zhou, J. Polariton-Assisted Singlet Fission in Acene Aggregates. *J. Phys. Chem. Lett.* **2018**, *9*, 1951−1957.
(43) Song, J.-H.; He, Y.; Nurmikko, A. V.; Tischler, J.; Bulovic, V. Exciton-Polariton Dynamics in a Transparent Organic Semiconductor Microcavity. *Phys. Rev. B: Condens. Matter Mater. Phys.* **2004**, *69*, 235330.
(44) Hobson, P. A.; Barnes, W. L.; Lidzey, D. G.; Gehring, G. A.; Whittaker, D. M.; Skolnick, M. S.; Walker, S. Strong Exciton-Photon Coupling in a Low-Q All-Metal Mirror Microcavity. *Appl. Phys. Lett.* **2002**, *81*, 3519−3521.
(45) Steger, M.; Liu, G.; Nelsen, B.; Gautham, C.; Snoke, D. W.; Balili, R.; Pfeiffer, L.; West, K. Long-Range Ballistic Motion and Coherent Flow of Long-Lifetime Polaritons. *Phys. Rev. B: Condens. Matter Mater. Phys.* **2013**, *88*, 235314.
(46) Nelsen, B.; Liu, G.; Steger, M.; Snoke, D. W.; Balili, R.; West, K.; Pfeiffer, L. Dissipationless Flow and Sharp Threshold of a Polariton Condensate with Long Lifetime. *Phys. Rev. X* **2013**, *3*, 041015.
(47) Sanvitto, D.; Kéna-Cohen, S. The Road Towards Polaritonic Devices. *Nat. Mater.* **2016**, *15*, 1061.
(48) Huo, P.; Coker, D. F. Communication: Partial Linearized Density Matrix Dynamics for Dissipative, Non-Adiabatic Quantum Evolution. *J. Chem. Phys.* **2011**, *135*, 201101.
(49) Lee, M. K.; Huo, P.; Coker, D. F. Semiclassical Path Integral Dynamics: Photosynthetic Energy Transfer with Realistic Environment Interactions. *Annu. Rev. Phys. Chem.* **2016**, *67*, 639−668.
(50) Huo, P.; Miller, T. F.; Coker, D. F. Communication: Predictive Partial Linearized Path Integral Simulation of Condensed Phase Electron Transfer Dynamics. *J. Chem. Phys.* **2013**, *139*, 151103.
(51) Huo, P.; Miller, T. F. Electronic Coherence and the Kinetics of Inter-Complex Energy Transfer in Light-Harvesting Systems. *Phys. Chem. Chem. Phys.* **2015**, *17*, 30914−30924.
(52) Castellanos, M. A.; Huo, P. Enhancing Singlet Fission Dynamics by Suppressing Destructive Interference between Charge-Transfer Pathways. *J. Phys. Chem. Lett.* **2017**, *8*, 2480−2488.
(53) Mandal, A.; Shakib, F. A.; Huo, P. Investigating Photoinduced Proton Coupled Electron Transfer Reaction Using Quasi Diabatic Dynamics Propagation. *J. Chem. Phys.* **2018**, *148*, 244102.
(54) Mandal, A.; Sandoval, J. S.; Shakib, F. A.; Huo, P. Quasi-Diabatic Propagation Scheme for Direct Simulation of Proton Coupled Electron Transfer Reaction. *J. Phys. Chem. A* **2019**, *123*, 2470.
(55) Mandal, A.; Yamijala, S.; Huo, P. Quasi Diabatic Representation for Nonadiabatic Dynamics Propagation. *J. Chem. Theory Comput.* **2018**, *14*, 1828−1840.
(56) Sandoval, C. J. S.; Mandal, A.; Huo, P. Symmetric Quasi Classical Dynamics with Quasi Diabatic Propagation Scheme. *J. Chem. Phys.* **2018**, *149*, 044115.
(57) Flick, J.; Narang, P. Cavity-Correlated Electron-Nuclear Dynamics from First Principles. *Phys. Rev. Lett.* **2018**, *121*, 113002.
(58) Jestadt, R.; Ruggenthaler, M.; Micael; Oliveira, J. T.; Rubio, A.; Appel, H. Real-Time Solutions of Coupled Ehrenfest-Maxwell-Pauli-Kohn-Sham Equations: Fundamentals, Implementation, and Nano-Optical Applications. *arXiv:1812.05049v2*, 2018.
(59) Flick, J.; Welakuh, D. M.; Ruggenthaler, M.; Appel, H.; Rubio, A. Light-Matter Response in Non-Relativistic Quantum Electrodynamics: Quantum Modifications of Maxwells Equations. *arXiv:1803.02519v2*, 2019.
(60) Chen, H.-T.; Li, T. E.; Sukharev, M.; Nitzan, A.; Subotnik, J. E. Ehrenfest+R Dynamics. I. a Mixed Quantum-Classical Electrodynamics Simulation of Spontaneous Emission. *J. Chem. Phys.* **2019**, *150*, 044102.
(61) Li, T. E.; Chen, H.-T.; Subotnik, J. E. Comparison of Different Classical, Semiclassical, and Quantum Treatments of Light-Matter Interactions: Understanding Energy Conservation. *J. Chem. Theory Comput.* **2019**, *15*, 1957−1973.
(62) Townsend, D.; Sussman, B. J.; Stolow, A. A Stark Future for Quantum Control. *J. Phys. Chem. A* **2011**, *115*, 357−373.
(63) Franco, I.; Shapiro, M.; Brumer, P. Robust Ultrafast Currents in Molecular Wires through Stark Shifts. *Phys. Rev. Lett.* **2007**, *99*, 126802.
(64) Schiffrin, A.; et al. Optical-Field-Induced Current in Dielectrics. *Nature* **2013**, *493*, 70−74.
(65) Garzón-Ramírez, A. J.; Franco, I. Stark Control of Electrons Across Interfaces. *Phys. Rev. B: Condens. Matter Mater. Phys.* **2018**, *98*, No. 121305R.
(66) Chikkaraddy, R.; de Nijs, B.; Benz, F.; Barrow, S. J.; Scherman, O. A.; Rosta, E.; Demetriadou, A.; Fox, P.; Hess, O.; Baumberg, J. J.

DOI: 10.1021/acs.jpclett.9b01599
J. Phys. Chem. Lett. 2019, 10, 5519−5529

Single-Molecule Strong Coupling at Room Temperature in Plasmonic Nanocavities. *Nature* **2016**, *535*, 127−130.
(67) Vahala, K. J. Optical Microcavities. *Nature* **2003**, *424*, 839−846.
(68) Smith, M. B.; Michl, J. Recent Advances in Singlet Fission. *Annu. Rev. Phys. Chem.* **2013**, *64*, 361−386.
(69) Berkelbach, T. C.; Hybertsen, M. S.; Reichman, D. R. Microscopic Theory of Singlet Exciton Fission. Ii. Application to Pentacene Dimers and the Role of Superexchange. *J. Chem. Phys.* **2013**, *138*, 114103.
(70) Haroche, S.; Kleppner, D. Cavity Quantum Electrodynamics. *Phys. Today* **1989**, *42*, 24.
(71) Scully, M. O.; Svidzinsky, A. A. The Lamb Shift—Yesterday, Today, and Tomorrow. *Science* **2010**, *328*, 1239−1241.
(72) Das, S.; Agarwal, G. S.; Scully, M. O. Quantum Interferences in Cooperative Dicke Emission from Spatial Variation of the Laser Phase. *Phys. Rev. Lett.* **2008**, *101*, 153601.
(73) Sapirstein, J. Quantum Electrodynamics of Many-Electron Atoms. *Phys. Scr.* **1987**, *36*, 801−808.
(74) Di Stefano, O.; Settineri, A.; Macrì, V.; Ridolfo, A.; Stassi, R.; Kockum, A. F.; Savasta, S.; Nori, F. Interaction of Mechanical Oscillators Mediated by the Exchange of Virtual Photon Pairs. *Phys. Rev. Lett.* **2019**, *122*, 030402.
(75) Stassi, R.; Macri, V.; Kockum, A. F.; Stefano, O. D.; Miranowicz, A.; Savasta, S.; Nori, F. Quantum Nonlinear Optics Without Photons. *Phys. Rev. A: At., Mol., Opt. Phys.* **2017**, *96*, 023818.

DOI: 10.1021/acs.jpclett.9b01599
J. Phys. Chem. Lett. 2019, 10, 5519−5529